[**Article ID**] 1003－6326(2001)02－0301－06

Dynamic model for landsliding monitoring under rigid body assumption①

ZHU Jian-jun(朱建军)[1], DING Xiao-li(丁晓利)[2], CHEN Yong-qi(陈永奇)[2]
(1. Department of Surveying Engineering, Central South University, Changsha 410083, P.R.China;
2. Department of Land Surveying and Geo-Informatics, Hong Kong Polytechnic University, Kowloon, Hong Kong)

[**Abstract**] Based on the assumption that the slope bodies are rigid, the dynamic model of the landsiding (forward model) was put forward. According to the dynamic model, the system equations of Kalman filter were constituted. The mechanical status of a slope was hence combined with the monitoring data by Kalman filter. The model uncertainties or model errors could also be considered through some fictitious observation equations. Different from existed methods, the presented method can make use for not only the statistic information contained in the data but also the information provided by the mechanical and geological aspect of slopes. At last a numerical example was given out to show the feasibility of the method.

[**Key words**] dynamic model; Kalman filter; rigid body; landslide monitoring
[**CLC number**] U416.1^{+}4; P207 [**Document code**] A

1 INTRODUCTION

Landslide is a main cause of the natural disaster. In order to prevent the disaster caused by landslide, a lot of slope monitoring were carried out, hence a lot of methods have been proposed to analyze the data collected through slope monitoring[1]. But most of these methods were based on statistics, for example, the regression-type methods, the time series-type methods which were based on the theory of time series and the grey theory-type methods which were developed in the recent decades[2~4]. Only the statistic information is used in these methods. The mechanical and geological aspect of slopes is not taken into consideration. No matter how the mechanical status and the geological conditions are, the same models will be used in these methods. These methods are effective at times. But misleading results can also be obtained due to the ignorance of the actual mechanical properties.

Another kind of methods is that of determinant model[1,5]. This kind of methods were based on the mechanics, but they work mainly in spatial domain. It is very difficult for them to be used in dynamic process (in time domain).

This paper describes a method that can make use of both the information provided by monitoring data as the statistic methods do and the information provided by the mechanical status of the slope body. The monitoring data and the mechanical status of the slope are combined with Kalman filter.

Based on the assumption that the slope bodies are rigid and the bodies keep touch with each other, the paper at first establishes the dynamic model of the landsliding (forward model). According to the dynamic model, the system equations of Kalman filter are constituted. The mechanical status of a slope is hence combined with the monitoring data by Kalman filter. The model uncertainties or model errors can also be considered through some fictitious observation equations. The concept is demonstrated through a simple slope sliding example.

2 DYNAMIC MODEL OF SLOPE

The slopes typically vary in the plane, wedge, curve or toppling modes[6]. If only the plane problem is concerned with, the plane, wedge and curve modes can be described as a block system (Fig.1)[7], that is, the fallen portion of a slope can usually be divided into a number of blocks.

Without loss of generality, only the system of blocks like that showed in Fig. 1 will be discussed in

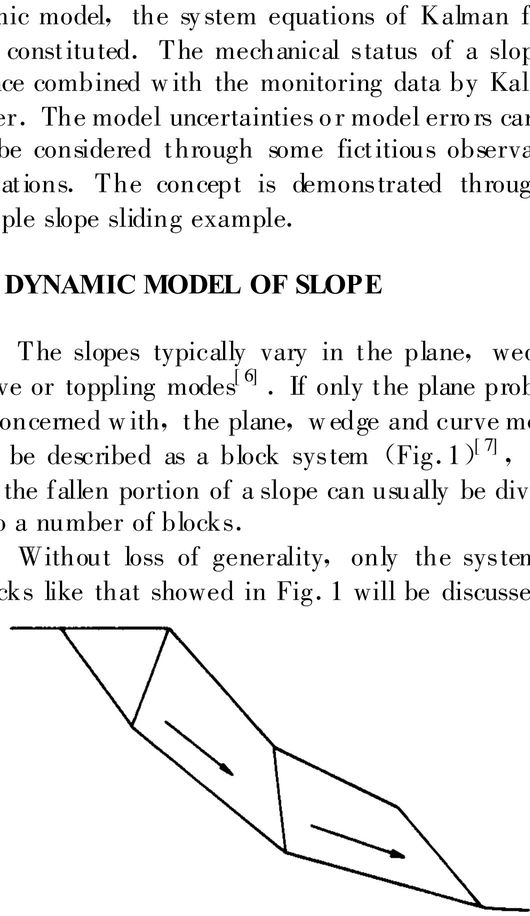

Fig.1 Block failure system

① [**Foundation item**] Project (49774209) supported by the National Natural Science Foundation of China

[**Received date**] 2000－05－26; [**Accepted date**] 2000－10－09

this paper. To simplify the problem, the blocks are considered as rigid bodies in the study.

If the geometry and material properties (e.g., coefficient of friction and unit weight) of a block system are known, the motion of the system can be derived.

From the Newton's second law of motion, the motion of any block can be described by (Fig. 2):

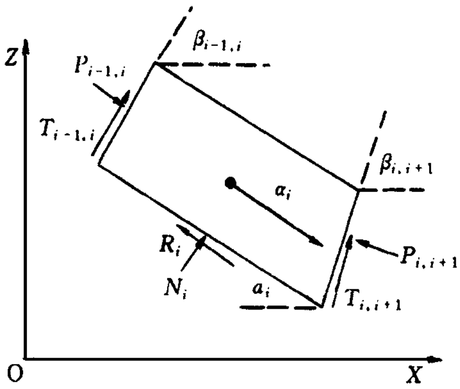

Fig. 2 Geometry and forces associated with rigid block

$$\left.\begin{aligned} m_i a_{ix} &= N_{ix} + R_{ix} + P_{i,(i-1)x} + P_{i,(i+1)x} + \\ &\quad T_{i,(i-1)x} + T_{i,(i+1)x} \\ m_i a_{iz} &= N_{iz} + R_{iz} + P_{i,(i-1)z} + P_{i,(i+1)z} + \\ &\quad T_{i,(i-1)z} + T_{i,(i+1)z} - m_i g \end{aligned}\right\} \tag{1}$$

where a_x, a_z are accelerations of the mass centre of the ith sliding block, that is

$$a_{ix} = \frac{\partial^2 x_i}{\partial t^2},\quad a_{iz} = \frac{\partial^2 z_i}{\partial t^2} \tag{2}$$

N is the normal force exerted on the surface of the block by the stable part of the slope; R is the resistant force as a result of the friction; N_x, N_z, R_x, R_z are the components of N and R in x and z directions respectively; m is the mass of the block; g is the acceleration due to gravity; x_i and z_i are the displacements of the block; P and T are the corresponding forces from the adjacent blocks; and t is the time. Eqn. (1) can also be written as

$$\boldsymbol{M}_i \boldsymbol{a}_i = \boldsymbol{A}_{1i} \boldsymbol{Y}_i + \boldsymbol{F}_i \tag{3}$$

where

$$\boldsymbol{A}_{1i} = \begin{pmatrix} \sin\alpha_i & -\cos\alpha_i & \sin\beta_{i,i-1} & -\sin\beta_{i,i-1} & -\cos\beta_{i,i-1} & -\cos\beta_{i,i+1} \\ \cos\alpha_i & \sin\alpha_i & -\cos\beta_{i,i-1} & \cos\beta_{i,i+1} & -\sin\beta_{i,i-1} & \sin\beta_{i,i+1} \end{pmatrix}$$

$$\boldsymbol{Y}_i = (N_i\ R_i\ P_{i-1,i}\ P_{i,i+1}\ T_{i-1,i}\ T_{i,i+1})^{\mathrm{T}}$$

$$\boldsymbol{M}_i = \begin{pmatrix} m_i & 0 \\ 0 & m_i \end{pmatrix}$$

$$\boldsymbol{a}_i = (a_{xi}\quad a_{zi})^{\mathrm{T}}$$

$$\boldsymbol{F}_i = (0 - m_i g)^{\mathrm{T}} \tag{4}$$

For the entire system of blocks, a general equation of Eqn. (3) can be formed:

$$\boldsymbol{M}\boldsymbol{a} = \boldsymbol{A}_1 \boldsymbol{Y} + \boldsymbol{G} \tag{5}$$

where

$$\boldsymbol{Y} = (N_1, N_2, \Lambda N_i \Lambda, R_1, \Lambda, R_1, \Lambda, P_{1,2}, \Lambda P_{i,i+1}, \Lambda P_{n-1,n}, T_{1,2}, \Lambda, T_{i,i+1}, \Lambda, T_{n-1,n})^{\mathrm{T}}$$

$$\boldsymbol{a} = (a_{x1}, a_{z1}, \Lambda a_{xi}, a_{zi}, \Lambda, a_{xn}, a_{z,n})^{\mathrm{T}}$$

$$\boldsymbol{G} = (0, m_1 g, \Lambda 0, m_i g, \Lambda, 0, m_n g)^{\mathrm{T}}$$

$\boldsymbol{M}$ and $\boldsymbol{A}_1$ are formed according to $\boldsymbol{M}_i$ and $\boldsymbol{A}_{1i}$ respectively.

Eqn. (5) describes the motion of a system of rigid body blocks. Obviously, if only one block is considered, then

$$\boldsymbol{Y} = \begin{pmatrix} N \\ R \end{pmatrix},\quad \boldsymbol{G} = \begin{pmatrix} 0 \\ mg \end{pmatrix},\quad \boldsymbol{A}_1 = \begin{pmatrix} \sin\alpha & -\cos\alpha \\ \cos\alpha & \sin\alpha \end{pmatrix} \tag{6}$$

Under the assumption of rigidity of the blocks and the constraints of the geometry, any block must move along the surface of discontinuities. This means that for any block, there must exist

$$a_{xi} \tan\alpha_i + a_{zi} = 0 \tag{7}$$

If there are n blocks in the system, there must be n such equations.

Besides, the displacements, velocities and accelerations of two adjacent blocks are assumed the same in directions normal to the surfaces of discontinuity. Therefore, for acceleration, there exists

$$a_{xi}\sin\alpha_{i,i+1} - a_{zi}\cos\alpha_{i,i+1} = a_{x(i+1)}\sin\alpha_{i,i+1} - a_{z(i+1)}\cos\alpha_{i,i+1} \tag{8}$$

If there are n blocks in the system, there must exist $n-1$ such equations. As for the block system, Eqns. (7) and (8) can be combined into

$$\boldsymbol{A}_2 \boldsymbol{a} = 0 \tag{9}$$

where $\boldsymbol{A}_2$ can be formed according to Eqns. (7) and (8).

The friction forces depend on the normal forces, i.e.,

$$\left.\begin{aligned} R_i &= kN_i + c \\ T_i &= kP_i + c \end{aligned}\right\} \tag{10}$$

where k is the coefficient of friction; and c is the force due to cohesion. For a system of n blocks, there must exist $2n-1$ such equations. The equations can be expressed as

$$\boldsymbol{A}_3 \boldsymbol{Y} = \boldsymbol{C} \tag{11}$$

Finally, the equations in (5), (9) and (11) can be expressed as

$$\boldsymbol{A}\boldsymbol{X} = \boldsymbol{L} \tag{12}$$

where

$$\boldsymbol{A} = \begin{pmatrix} -\boldsymbol{M} & \boldsymbol{A}_1 \\ \boldsymbol{A}_2 & 0 \\ 0 & \boldsymbol{A}_3 \end{pmatrix},\quad \boldsymbol{L} = \begin{pmatrix} -\boldsymbol{G} \\ 0 \\ \boldsymbol{C} \end{pmatrix},\quad \boldsymbol{X} = \begin{pmatrix} \boldsymbol{a} \\ \boldsymbol{Y} \end{pmatrix}$$

There are $6n-2$ unknowns and $6n-2$ equations in Eqn. (12). Therefore the equations have unique solutions. Muliplying Eqn. (12) by $\boldsymbol{A}^{\mathrm{T}}$, one gets

$$\boldsymbol{A}^{\mathrm{T}}\boldsymbol{A}\boldsymbol{X} = \boldsymbol{A}^{\mathrm{T}}\boldsymbol{L} \tag{13}$$

and

$$\boldsymbol{X} = (\boldsymbol{A}^{\mathrm{T}}\boldsymbol{A})^{-1}\boldsymbol{A}^{\mathrm{T}}\boldsymbol{L} \tag{14}$$

Eqn. (14) can be easy to solve by many existed softwares for surveying adjustment. After the accelerations are found from the above, one can derive the motion velocity and displacement of the slope using

$$\left.\begin{aligned} V_{xi} &= \frac{\partial X_i}{\partial t} = \int a_{xi}\mathrm{d}t, \\ V_{zi} &= \frac{\partial Z_i}{\partial t} = \int a_{zi}\mathrm{d}t \end{aligned}\right\} \quad (15a)$$

$$X_i = \iint a_{xi}\mathrm{d}t\mathrm{d}t,\ Z_i = \iint a_{zi}\mathrm{d}t\mathrm{d}t \quad (15b)$$

In a small time step, one can get:

$$\left.\begin{aligned} V_{xi} &= V_{xio} + a_{xi}t \\ V_{zi} &= V_{zio} + a_{zi}t \\ X_i &= X_{io} + V_{xio}t + t^2 a_{xi}/2 \\ Z_i &= Z_{io} + V_{zio}t + t^2 a_{zi}/2 \end{aligned}\right\} \quad (16)$$

Eqns. (12), (15) and (16) constitute the forward model of the slope. Based on the known geometry and material properties, one can find the displacement of the slope.

If Eqn. (12) is used directly, double precision variables are needed to use in programming since most numbers need at least 16 digits. In order to improve the computation accuracy and make the numerical computation stable, we make a transformation of parameters $\boldsymbol{Y}$. Let

$$\boldsymbol{Y} = \boldsymbol{Y}_0 + \Delta\boldsymbol{Y}$$

where $\boldsymbol{Y}_0$ is the value of $\boldsymbol{Y}$ when in the state of limiting equilibrium. Since the acceleration of any slope body will be $a_{xi} = a_{zi} = 0$ in an equilibrium state, from Eqns. (5) and (11), one can get

$$\left.\begin{aligned} \boldsymbol{A}_1\boldsymbol{Y}_0 + \boldsymbol{G}_0 &= 0 \\ \boldsymbol{A}_3\boldsymbol{Y}_0 &= \boldsymbol{C}_0 \end{aligned}\right\} \quad (17)$$

$\boldsymbol{G}_0$, $\boldsymbol{C}_0$ is the values of $\boldsymbol{G}$ and $\boldsymbol{C}$ in the limiting equilibrium state. Substituting Eqn. (17) into Eqn. (12), the equation becomes

$$\begin{pmatrix} -\boldsymbol{M} & \boldsymbol{A}_1 \\ \boldsymbol{A}_2 & 0 \\ 0 & \boldsymbol{A}_3 \end{pmatrix}\begin{pmatrix} \boldsymbol{a} \\ \Delta\boldsymbol{Y} \end{pmatrix} = \begin{pmatrix} -\Delta\boldsymbol{G} \\ 0 \\ \Delta\boldsymbol{C} \end{pmatrix} \quad (18)$$

where

$$\Delta\boldsymbol{Y} = \boldsymbol{Y} - \boldsymbol{Y}_0,\ \Delta\boldsymbol{C} = \boldsymbol{C} - \boldsymbol{C}_0$$

$$\Delta\boldsymbol{G} = \boldsymbol{G} - \boldsymbol{G}_0 = (0,\ \Delta m_1 g,\ \Lambda,\ 0,\ \Delta m_i g,\ \Lambda)$$

In order to keep symbols simple, we will still use

$$\boldsymbol{X} = \begin{pmatrix} \boldsymbol{a} \\ \Delta\boldsymbol{Y} \end{pmatrix},\ \boldsymbol{L} = \begin{pmatrix} -\Delta\boldsymbol{G} \\ 0 \\ \Delta\boldsymbol{C} \end{pmatrix}$$

in the rest of the paper. Eqn. (18) can still be written as

$$\boldsymbol{AX} = \boldsymbol{L} \quad (19)$$

It is obvious that $\Delta\boldsymbol{Y}$ describes the difference between the present state and the stable state.

3 KALMAN FILTER MODEL

The state of a sliding slope can be described by the following state vector,

$$\boldsymbol{X} = (\boldsymbol{X}_1^{\mathrm{T}},\ \boldsymbol{V}^{\mathrm{T}},\ \boldsymbol{a}^{\mathrm{T}},\ \Delta\boldsymbol{Y}^{\mathrm{T}})^{\mathrm{T}} \quad (20)$$

where

$$\boldsymbol{X}_1 = (x_1,\ z_1,\ \Lambda,\ x_i,\ z_i\Lambda)^{\mathrm{T}}$$

$$\boldsymbol{V} = \boldsymbol{X}_1^{\&} = (v_{x1},\ v_{z1},\ \Lambda,\ v_{xi},\ v_{zi},\ \Lambda)^{\mathrm{T}}$$

$$\boldsymbol{a} = \boldsymbol{V}^{\&} = (a_{x1},\ a_{z1},\ \Lambda,\ a_{xi},\ a_{zi},\ \Lambda)^{\mathrm{T}}$$

$\boldsymbol{X}_1$ is the vector of displacements, $\boldsymbol{V}$ is the vector of velocities.

Four different state transition models can be derived:

1) The first one is based on the rigid body motion equation and on the forward analysis model. According to the rigid body motion equation, when the state transits from state k to state $k+1$, the displacement and the velocity will change to:

$$\left.\begin{aligned} \boldsymbol{X}_{1,k+1} &= \boldsymbol{X}_{1,k} + t\boldsymbol{V}_k + t^2\boldsymbol{a}_k/2 \\ \boldsymbol{V}_{1,k+1} &= \boldsymbol{V}_k + t\boldsymbol{a}_k \end{aligned}\right\} \quad (21)$$

In real situations, the external forces acting on a slope body usually will not change except when for example the ground water level changes after rains or ground shaking is induced by earthquakes. Therefore it is reasonable to assume $\Delta\boldsymbol{G} = 0$ and $\Delta\boldsymbol{Y}_{k+1} = \Delta\boldsymbol{Y}_k$. If there exists any change in the external forces, they can be considered as state transition errors (system noises) if the changes are not very significant. Based on this assumption and Eqn. (18), one can get

$$\left.\begin{aligned} \Delta\boldsymbol{Y}_{k+1} &= \Delta\boldsymbol{Y}_k \\ \boldsymbol{a}_{k+1} &= \boldsymbol{M}^{-1}\boldsymbol{A}_1\Delta\boldsymbol{Y}_{k+1} + \boldsymbol{M}^{-1}\Delta\boldsymbol{G} \\ &= \boldsymbol{M}^{-1}\boldsymbol{A}_1\Delta\boldsymbol{Y}_k \end{aligned}\right\} \quad (22)$$

Combining (21) with (22), we can get the following state transition equation:

$$\boldsymbol{X}_{k+1} = \Phi_k\boldsymbol{X}_k = \begin{pmatrix} I & tI & t^2I/2 & 0 \\ 0 & I & tI & 0 \\ 0 & 0 & 0 & \boldsymbol{M}^{-1}\boldsymbol{A}_1 \\ 0 & 0 & 0 & I \end{pmatrix}\begin{pmatrix} \boldsymbol{X}_{1,k} \\ \boldsymbol{V}_k \\ \boldsymbol{a}_k \\ \Delta\boldsymbol{Y}_k \end{pmatrix} \quad (23)$$

2) The second state transition model is based on the forward analysis model only. The time-dependent state equation is

$$\boldsymbol{X}^{\&} = \begin{pmatrix} \boldsymbol{X}_1^{\&} \\ \boldsymbol{V}^{\&} \\ \boldsymbol{a}^{\&} \\ \Delta\boldsymbol{Y}^{\&} \end{pmatrix} = \begin{pmatrix} \boldsymbol{V} \\ \boldsymbol{a} \\ 0 \\ 0 \end{pmatrix} = \begin{pmatrix} \boldsymbol{V} \\ \boldsymbol{M}^{-1}\boldsymbol{A}_1\Delta\boldsymbol{Y} + \Delta\boldsymbol{G} \\ 0 \\ 0 \end{pmatrix} = \begin{pmatrix} \boldsymbol{V} \\ \boldsymbol{M}^{-1}\boldsymbol{A}_1\Delta\boldsymbol{Y} \\ 0 \\ 0 \end{pmatrix} = \begin{pmatrix} 0 & I & 0 & 0 \\ 0 & 0 & 0 & \boldsymbol{M}^{-1}\boldsymbol{A}_1 \\ 0 & 0 & 0 & 0 \\ 0 & 0 & 0 & 0 \end{pmatrix}\begin{pmatrix} \boldsymbol{X}_1 \\ \boldsymbol{V} \\ \boldsymbol{a} \\ \Delta\boldsymbol{Y} \end{pmatrix} \quad (24)$$

where

$$\boldsymbol{X}^{\&} = \frac{\partial\boldsymbol{X}}{\partial t},\ \boldsymbol{X}_1^{\&} = \frac{\partial\boldsymbol{X}_1}{\partial t},$$

$$\boldsymbol{a}^{\&} = \frac{\partial\boldsymbol{a}}{\partial t},\ \Delta\boldsymbol{Y}^{\&} = \frac{\partial\Delta\boldsymbol{Y}}{\partial t},\ \Delta\boldsymbol{G} = 0$$

By discretising the above continuous-time state equation using series expansions[8], a discrete-time state equation is obtained:

$$\boldsymbol{X}_{k+1}=\Phi_k\boldsymbol{X}_k=\begin{pmatrix} I & tI & 0 & t^2\boldsymbol{M}^{-1}\boldsymbol{A}_1/2 \\ 0 & I & 0 & t\boldsymbol{M}^{-1}\boldsymbol{A}_1 \\ 0 & 0 & I & 0 \\ 0 & 0 & 0 & I \end{pmatrix}\begin{pmatrix} \boldsymbol{X}_{1,k} \\ \boldsymbol{V}_k \\ \boldsymbol{a}_k \\ \Delta\boldsymbol{Y}_k \end{pmatrix} \tag{25}$$

3) The third model is an improved form of the second. The model given in Eqn. (25) above can be substituted by

$$\boldsymbol{X}_{k+1}=\Phi_k\boldsymbol{X}_k=\begin{pmatrix} I & tI & t^2\boldsymbol{M}^{-1}\boldsymbol{A}_1/2 \\ 0 & I & t\boldsymbol{M}^{-1}\boldsymbol{A}_1 \\ 0 & 0 & I \end{pmatrix}\begin{pmatrix} \boldsymbol{X}_{1,k} \\ \boldsymbol{V}_k \\ \Delta\boldsymbol{Y}_k \end{pmatrix} \tag{26}$$

that is, in this model

$$\boldsymbol{X}=\begin{pmatrix} \boldsymbol{X}_1 \\ \boldsymbol{V} \\ \Delta\boldsymbol{Y} \end{pmatrix}$$

This means that the third model is the same as the second, but has less parameters in the state vector. The model is therefore simpler.

4) The last model is the one widely used in kinetic systems. In this model, only the rigid motion equation is considered[9],

$$\boldsymbol{X}_{k+1}=\Phi_k\boldsymbol{X}_k=\begin{pmatrix} I & tI & t^2 I/2 \\ 0 & I & t_1 I \\ 0 & 0 & I \end{pmatrix}\begin{pmatrix} \boldsymbol{X}_{1,k} \\ \boldsymbol{V}_k \\ \boldsymbol{a}_k \end{pmatrix} \tag{27}$$

The stochastic state transition equation is obtained if the state transition errors (the system noises) w are added to Eqns. (23), (25), (26) or (27):

$$\boldsymbol{X}_{k+1}=\Phi_k\boldsymbol{X}_k+w \tag{28}$$

Any of the above four models can be used as the state equation in Kalman filter. In the following section we will discuss which will be the best.

In slope deformation monitoring, observation equations can be established for all the observations,

$$\boldsymbol{L}_1=\boldsymbol{B}_1\boldsymbol{X}+\varepsilon_1 \tag{29}$$

where

$$\boldsymbol{B}_1=(I \quad 0 \quad 0)$$

and $\boldsymbol{L}_1$ denotes the observations vector, ε_1 is the observations error vector. Under the assumption that the slope bodies are rigid, one can establish some constraints. For example, according to the forward model (18), we have

$$\left.\begin{aligned} \boldsymbol{A}_2\boldsymbol{a}_{k+1}&=0 \\ \boldsymbol{A}_3\Delta\boldsymbol{Y}_{k+1}&=\Delta\boldsymbol{C} \end{aligned}\right\} \tag{30}$$

These can be used as geometric constraints. Besides, the displacements and velocities of the two blocks that are adjacent to each other must be the same in the normal direction of the contact surface. Therefore, similar to Eqn. (9), the following should hold:

$$\left.\begin{aligned} \boldsymbol{A}_2\boldsymbol{X}_{1,k+1}&=0 \\ \boldsymbol{A}_2\boldsymbol{V}_{k+1}&=0 \end{aligned}\right\} \tag{31}$$

Eqns. (30) and (31) can be rewritten as

$$\boldsymbol{B}_2\boldsymbol{X}_{k+1}=\boldsymbol{L}_2 \tag{32}$$

where

$$\boldsymbol{B}_2=\begin{pmatrix} \boldsymbol{A}_2 & 0 & 0 & 0 \\ 0 & \boldsymbol{A}_2 & 0 & 0 \\ 0 & 0 & \boldsymbol{A}_2 & 0 \\ 0 & 0 & 0 & \boldsymbol{A}_3 \end{pmatrix},\quad \boldsymbol{L}_2=\begin{pmatrix} 0 \\ 0 \\ 0 \\ \Delta\boldsymbol{G} \end{pmatrix}$$

In the real situations, Eqn. (32) may not be completely satisfied due to the errors caused by the assumptions. For example, the blocks will always more or less deform and therefore are not exactly rigid. Besides, the failure surfaces may also be known only approximately. One better way to treat the constraints is to consider them as observations with certain uncertainties,

$$\boldsymbol{B}_2\boldsymbol{X}_{k+1}=\boldsymbol{L}_2+\varepsilon_2 \tag{33}$$

where ε_2 is an error term. The above equations can be used as observation equations.

Based on Eqn. (28), we can get the following Kalman filter model

$$\boldsymbol{X}_{k+1}=\Phi_k\boldsymbol{X}_k+w \tag{34}$$

$$\boldsymbol{L}_{k+1}=\boldsymbol{B}\boldsymbol{X}_{k+1}+\varepsilon\boldsymbol{P}_{k+1} \tag{35}$$

$$\boldsymbol{B}=\begin{pmatrix} \boldsymbol{B}_1 \\ \boldsymbol{B}_2 \end{pmatrix},\quad \boldsymbol{L}_{k+1}=\begin{pmatrix} \boldsymbol{L}_{1,k+1} \\ \boldsymbol{L}_2 \end{pmatrix},$$

$$\boldsymbol{P}_{k+1}=\begin{pmatrix} \boldsymbol{P}_L & 0 \\ 0 & \boldsymbol{P}_{\varepsilon_2} \end{pmatrix},\quad \varepsilon=\begin{pmatrix} \varepsilon_1 \\ \varepsilon_2 \end{pmatrix}$$

The computation formulae of Kalman filter are[9]

$$\left.\begin{aligned} \overline{\boldsymbol{X}}_{k+1}&=\Phi_k\boldsymbol{X}_k \\ \boldsymbol{Q}_{\overline{X}_{k+1}}&=\Phi_k\boldsymbol{Q}_{X_k}\Phi_k^{\mathrm{T}}+\boldsymbol{Q}_w \\ \boldsymbol{X}_{k+1}&=\overline{\boldsymbol{X}}_{k+1}+\boldsymbol{Q}_{\overline{X}_{k+1}}\boldsymbol{B}^{\mathrm{T}}(\boldsymbol{B}\boldsymbol{Q}_{\overline{X}_{k+1}}\boldsymbol{B}^{\mathrm{T}}+ \\ &\quad \boldsymbol{Q}_{k+1})^{-1}(\boldsymbol{L}_{k+1}-\boldsymbol{B}\overline{\boldsymbol{X}}_{k+1}) \\ \boldsymbol{Q}_{X_{k+1}}&=\boldsymbol{Q}_{\overline{X}_{k+1}}-\boldsymbol{Q}_{\overline{X}_{k+1}}\boldsymbol{B}^{\mathrm{T}}(\boldsymbol{B}\boldsymbol{Q}_{\overline{X}_{k+1}}\boldsymbol{B}^{\mathrm{T}}+ \\ &\quad \boldsymbol{Q}_{k+1})^{-1}\boldsymbol{B}\overline{\boldsymbol{X}}_{k+1} \end{aligned}\right\} \tag{36}$$

or[10]

$$\left.\begin{aligned} \boldsymbol{X}_{k+1}&=\overline{\boldsymbol{X}}_{k+1}+\boldsymbol{J}(\boldsymbol{L}_k-\boldsymbol{B}\overline{\boldsymbol{X}}_{k+1}) \\ \boldsymbol{Q}_{X_{k+1}}&=(I-\boldsymbol{J}\boldsymbol{B})\boldsymbol{Q}_{\overline{X}_{k+1}} \\ \boldsymbol{J}&=\boldsymbol{Q}_{\overline{X}_{k+1}}\boldsymbol{B}^{\mathrm{T}}(\boldsymbol{B}\boldsymbol{Q}_{\overline{X}_{k+1}}\boldsymbol{B}^{\mathrm{T}}+\boldsymbol{Q}_{k+1})^{-1} \end{aligned}\right\} \tag{37}$$

where

$$\boldsymbol{Q}_{k+1}=\boldsymbol{P}_{k+1}^{-1},\quad \boldsymbol{Q}_w=\boldsymbol{P}_w^{-1}$$

In practical computations, two problems must be considered when the above formulae are used, i. e., the initial values of $\boldsymbol{X}$, and the variances of the system errors w and the model errors ε_2 (or the model uncertainty). The initial values of $\boldsymbol{X}$ can be determined by using the condition of limiting equilibrium. If a slope has already begun to slide, the displacements, velocities and the accelerations can be determined by using initial two epochs of surveys.

4 NUMERICAL EXAMPLES

Stimulated examples are given here to show the feasibility of the Kalman filter model presented above. The block system used in the stimulated examples is similar to that shown in Fig. 1 and Fig. 3. The parameters of the system are taken as: $m_1=798$ t, $m_2=4$kt, $m_3=400$t, $\alpha_1=60$, $\alpha_2=45$, $\alpha_3=30$, $\beta_{12}=60$ and $\beta_{23}=75$, and the cohesion force $c=0$. The coefficient of friction k in the state of limiting equilibrium is $k=0.7670573627281236$. One observed point was placed on each of the three blocks, and observations of the horizontal and vertical displacements of the observed points were stimulated by computer. The observations were taken once every 5 days for one year period. The observation errors are given by computer. The variance of the stimulated errors is $\sigma^2=3^2\,\mathrm{mm}^2=9\,\mathrm{mm}^2$.

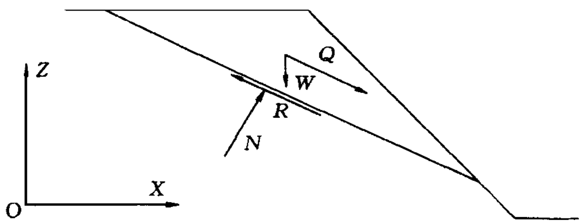

Fig. 3 Sliding block on plane

After the observations were taken, the Kalman filter model (23), (25), (26) and (27) were used respectively to process the stimulated data. Figs. 4, 5, 6 and 7 give the results from the different models. In these figures, the stimulated observations, the real displacements and values computed by the Kalman filter are given. Table 2 lists the following values for each of the Kalman filter models:

$$\left.\begin{aligned} \delta_\Sigma &= \sum (\hat{x}_k - \overline{x}_k)^2 \\ \sigma_k &= \sqrt{\frac{\delta_\Sigma}{n}} \end{aligned}\right\} \qquad (38)$$

where $\hat{x}_k$ and $\overline{x}_k$ are the filtered and the true displacements respectively, and n is the number of epoches.

It can be seen from Table 1 and the figures.

1) The results from the first three models are much more accurate than the original observed values. The variances decreased by 6 ($3^2/1.2262$) to 29 ($3^2/0.5562$).

2) The results from Eqn. (25) are the same as those from Eqn. (26). This means the two models are equivalent, but the computations using Eqn. (26) are simpler. The results from both Eqn. (25) and Eqn. (26) are better than those from Eqn. (23).

3) The results from Eqns. (23), (25) and (26) are all significantly better than those from Eqn. (27). This means that the Kalman filter based on the me

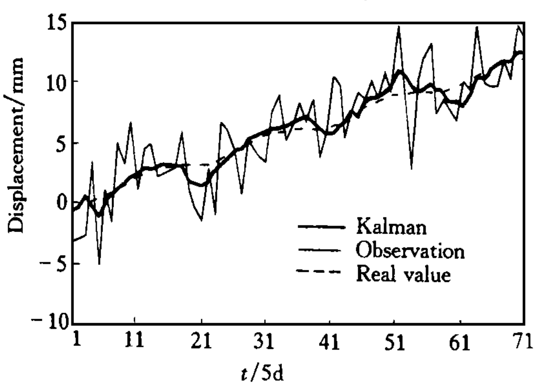

Fig. 4 Displacement curves from model 1

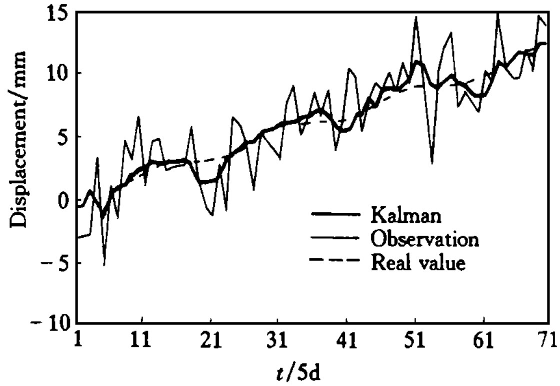

Fig. 5 Displacement curves from model 2

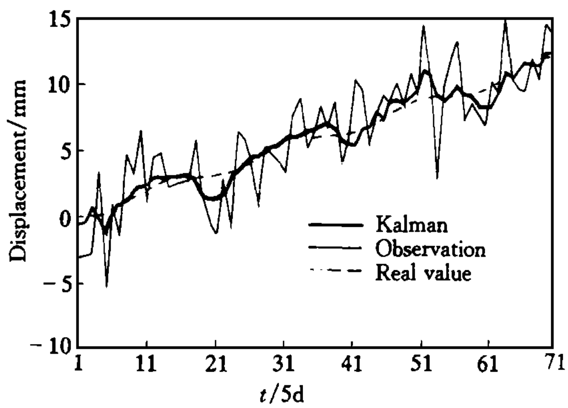

Fig. 6 Displacement curves from model 3

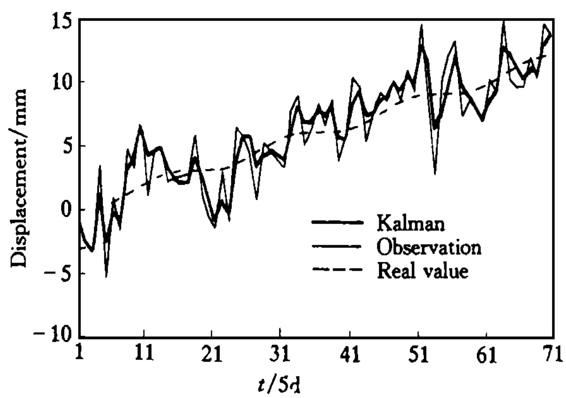

Fig. 7 Displacement curves from model 4

Table 2 Filtering deviations

Model	Parameter	X_1	Z_1	X_2	Z_2	X_3	Z_3
Model (1)	$\hat{\delta}_\Sigma$	35.06	105.15	56.32	56.34	67.93	22.68
	σ_Σ	0.708	1.226	0.897	0.897	0.985	0.568
Model (2)	$\hat{\delta}_\Sigma$	33.40	100.16	53.66	53.68	64.71	21.60
	σ_Σ	0.691	1.196	0.876	0.876	0.962	0.556
Model (3)	$\hat{\delta}_\Sigma$	33.40	100.16	53.66	53.68	64.71	21.60
	σ_Σ	0.961	1.196	0.876	0.876	0.962	0.556
Model (4)	$\hat{\delta}_\Sigma$	242.23	338.58	502.48	354.28	317.60	383.48
	σ_Σ	1.860	2.199	2.679	2.250	2.130	2.341

chanical model of the slope is significantly better.

5 CONCLUSIONS

1) Under the assumption that the slope bodies are rigid, the dynamic model of slope sliding is derived. If we can get the accurate mechanical parameters, we can derive the dynamic process of a slope deformation.

2) According to the dynamic model, the system equations of Kalman filter are constituted. The mechanical status of a slope is hence combined with the monitoring data by Kalman filter. Based on the principle of mechanics and existing Kalman filter approaches, four kinds of Kalman filter model are presented. The results show that the Kalman filter models based dynamic model is significantly better.

3) The uncertainty of the model or model error usually influence heavily on the results of analysis in many fields. In this paper, it is take into consideration by the additional fictitious observation equations.

4) As the mechanical properties of slopes vary considerably from one to another, more research is still required to take into account to study the special characteristics of the various types of slopes.

[REFERENCES]

[1] CHEN Y Q. The Data Processing Approach for Deformation Observation [M]. Beijing: Surveying and Mapping Publish House, 1988. 1—350.

[2] Chen Y Q and Tang Conrad. Application of the theory of grey theory system in the analysis of deformation surveyings [A]. 7th International FIG Symposium on Deformation Measurements [C]. 1993. 303—309.

[3] LIU Zu-qiang. Prediction of landsliding by grey theory [J]. Site Investigation Science and Technology, (in Chinese), 1991, 5: 1—5.

[4] YIN Hui. An application of time series analysis and grey theory in the deformation prediction at Lian Zi cliff [A]. The 8th FIG International Symposium on Deformation Measurements [C]. 25—28, June, 1996. Hong Kong, 1996, 267—274.

[5] Chrzanowski. Combination of Geometrical Analysis with Physical Interpretation for the Enhancement of Deformation Modelling [M]. FIG XIX International Congress, 612(3): 1—15.

[6] Hoek E and Bray J W. Rock Slope Engineering [M]. London: Institution of Mining and Metallurgy, 1981. 1—200.

[7] SHI G H. Block System Modelling by Discontinuous Deformation Analysis [M]. Southampton UK and Boston USA, Computational Mechanics Publications, 1993. 1—200.

[8] REN D and DING X. Dynamic deformation analysis of open pit slopes [A]. The 8th Fig International Symposium on Deformation Measurements [C]. 25—28, June, 1996, Hong Kong, 1996. 157—163.

[9] CHUI C K and CHEN G. Kalman Filtering with Real Time Applications [M]. Springer-Verlag, Berlin, New York, 1992. 1—250.

[10] Jia M, Ding X and Montgomery B. On reliability measures for kinetic surveys [J]. Geomatica, 1998, 52(1): 37—44.

(Edited by HUANG Jin-song)